Control of chaos by time–delayed feedback in high–power ferromagnetic resonance experiments

Hartmut Benner
Institut für Festkörperphysik, TU–Darmstadt, Hochschulstr. 6, D–64289 Darmstadt, Germany

Wolfram Just* †
Institut für Physik, TU–Chemnitz, D-09107 Chemnitz, Germany
(February 6, 2002)

Basic features of time–delayed feedback schemes for the control of chaos are reviewed. The method is applied to high–power ferromagnetic resonance experiments in YIG spheres beyond the Suhl threshold. Chaotic motion is suppressed and regular periodic states are stabilised.

Since the pioneering work on control of chaos [1] problems of control have developed to one of the most important topics in applied nonlinear sciences over the last decade [2]. Although control theory is a well developed discipline in engineering and applied mathematics (cf. e.g. [3,4]) the new aspects proposed by physicists concern the usage of non-invasive methods to stabilise one of numerous unstable states embedded in a chaotic system. A second milestone in this business concerns the usage of time–delayed measured signal to construct suitable control forces for stabilising time periodic states [5]. Such an approach can easily be applied even in complicated experiments [6,7] since neither a proper mathematical modelling of the internal dynamics nor a fancy data processing are required for employing the control scheme. Such conditions occur frequently in fast experimental systems.

Time–delayed feedback schemes use a measured signal $s(t)$ of the system and derive the control force from the time–delayed difference $s(t) - s(t - \tau)$. Here the delay time τ is chosen in such a way that it coincides with the period of the orbit to be stabilised, so that the control force finally vanishes when the target state is reached. The control scheme is sketched in figure 1. From the theoretical point of view the analysis of the control performance results in the discussion of delay systems which are a priori infinite dimensional even if their free dynamics is quite simple [8]. Thus a deeper understanding of the control properties has been developed only recently [9–11]. Employing a linear stability analysis the control performance can be reduced to characteristic exponents $\Lambda + i\Omega$ where successful control corresponds to negative values $\Lambda < 0$ for the real part. Under very general conditions [12] the characteristic equation determining the exponents can be written as

$$\Lambda + i\Omega = \lambda + i\omega + K(\chi' + i\chi'')(1 - \exp[-(\Lambda + i\Omega)\tau]) \quad . \quad (1)$$

Here $\lambda + i\omega$ denotes the stability exponent of the free orbit with $\lambda > 0$, and the parameter $\chi' + i\chi''$ takes all the details of the control scheme into account, i.e. the properties of the measured signal and the coupling of the control force.

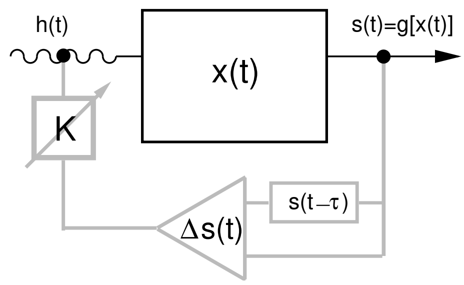

FIG. 1. Control scheme for time–delayed feedback control. The control loop is displayed in gray. The control force consists of the control signal $\Delta s(t) = s(t) - s(t - \tau)$ and the control amplitude K which acts as a linear amplification.

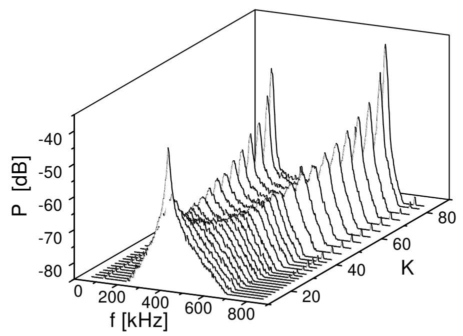

FIG. 2. Response spectrum of an electronic circuit subjected to delayed feedback control within the control domain ($\tau = 1.25\mu$s). Peaks are caused by the leading exponent.

*e–mail: wolfram.just@physik.tu-chemnitz.de
†permanent address: School of Mathematical Sciences, Queen Mary / Univ. of London, Mile End Road, London E1 4NS, UK

The stability exponents can be measured e.g. by applying linear response methods. Here one superimposes a small harmonic forcing and detects the control signal. Within the control interval the position and widths of the corresponding lines in the Fourier spectrum yield imaginary and real part of the stability exponents (cf. figure 2). The measured exponents can be compared with the theoretical prediction, eq.(1). Evaluation of the latter is quite straightforward (cf. [13]). One obtains a characteristic butterfly shaped curve for the real part which results in a finite control interval where $\Lambda < 0$. This behaviour is accompanied by a frequency splitting phenomenon for the imaginary part, caused by a collision of two distinct exponents. The general theory fits well with experimental results, even a quantitative coincidence up to 5% is observed.

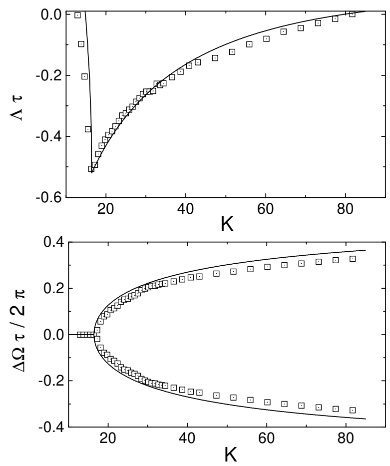

FIG. 3. Real part Λ and frequency deviation $\Delta\Omega = \Omega - \omega$ of the leading stability exponent in dependence on the control amplitude K for an electronic circuit experiment (cf. figure 2). Symbols: experimental results, line: numerical fit according to eq.(1) with $-\tau\chi' = 0.036$, $\chi'' = 0$ and $\lambda\tau = 1.07$, $\omega\tau = \pi$.

The typical shape of the leading eigenvalue yields a finite control interval with two thresholds, a lower and an upper critical control amplitude. At the lower threshold control sets in via a reverse flip bifurcation. Provided the bifurcation is supercritical one expects that in the Fourier spectrum of the measured signal a peak at half the basic frequency disappears when one enters the control interval on increasing K. Such a prediction is confirmed by experiments (cf. figure 4). At the upper threshold the eigenvalue spectrum develops a nontrivial imaginary part indicating a Hopf bifurcation. Thus sideband frequencies are visible in the Fourier spectrum of the signal. Both features are typical for time–delayed feedback methods.

The size of the control interval depends on properties of the free orbit, in particular on its Lyapunov exponent λ. For larger values of λ the spectrum displayed in figure 3 is essentially shifted upwards. A more thorough analysis shows [14], that the control interval vanishes for $\lambda\tau = 2$. Such a constraint limits the original scheme to weakly unstable orbits. Multiple delay times have proven to be fruitful to stabilise highly unstable periodic orbits [15]. The method is quite robust and easy to implement either by filtering the control signal electronically or by implementing multiple delays using the travelling time of signals, e.g. through a resonator in optical experiments.

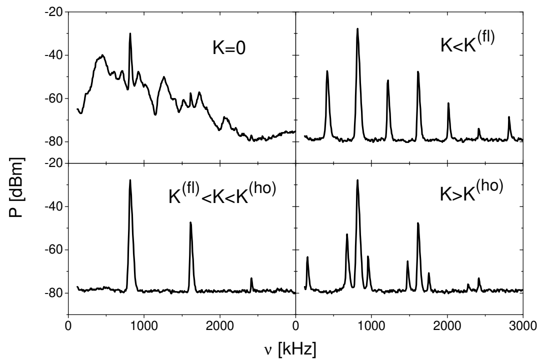

FIG. 4. Fourier spectrum of the measured signal, without control ($K = 0$: chaotic), below the lower critical control amplitude ($K < K^{(fl)}$: period two), within the control interval ($K^{(fl)} < K < K^{(ho)}$: periodic), and above the upper control threshold ($K > K^{(ho)}$: quasiperiodic).

A severe limitation of conventional delayed feedback schemes results from the fact that only orbits with a complex stability exponent can be stabilised [10,11]. This restriction can be relaxed by means of a time dependent modulation of the control amplitude K [16,17]. Such approaches have been successfully applied in experiments [16]. The method relies to some extent on the quite complicated structure of the eigenvalue spectrum which explores the infinite dimensionality of the phase space (cf. [18]). As an alternative control loops have been proposed recently which contain an additional unstable degree of freedom [19]. Although such an idea is to some extend known in control theory, its combination with time–delayed feedback methods is new and the scheme has not yet been applied in real experiments.

Time–delayed feedback methods do not require the knowledge of the orbit to be stabilised in advance. Several empirical and semiempirical schemes have been proposed to find suitable delay times from properties of the control signal [20,21]. These methods are essentially based on observing dominant peaks in the Fourier spectrum of the control signal and adjusting the delay time within an iteration process. Such schemes can be based on theoretical arguments by a proper analysis of the full delay system including the control force [22].

It is well known by engineers that control loop latency, i.e. the time lag needed for coupling the control force to the system under consideration, severely limits the efficiency of traditional control methods [23]. Such reservations apply for time–delayed feedback control as well, and one may quantitatively express such a constraint in terms of the control loop latency, the period of the orbit, and its Lyapunov exponent [24].

Altogether the mechanism of time–delayed feedback control is meanwhile well understood from the theoretical point of view. Here we are going to apply such concepts for controlling chaos in strongly driven magnetic systems. Magnetic systems are strongly nonlinear devices via the coupling of effective magnetic fields to the internal degrees of freedom. They are considered as paradigms for nonlinear dynamics and pattern forming systems, which are to date only poorly understood [25].

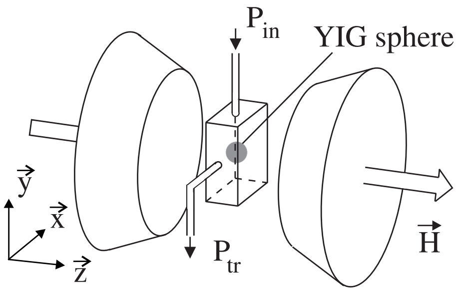

FIG. 5. Setup for the ferromagnetic resonance experiment.

High–power ferromagnetic resonance experiments were performed on spheres of yttrium iron garnet (YIG), which is well established as a "prototype nonlinear ferromagnet". The sample was placed in a microwave cavity and excited by a microwave field of 9.39 GHz, applied perpendicularly or parallel to the static magnetic field (cf. figure 5). The subsidiary absorption manifests as an additional absorption structure at lower field, which is well separated from the FMR main resonance and shows a drastic broadening with increasing microwave power, accompanied by auto–oscillations and sequences of bifurcations. We have systematically analysed [26] the dynamic behaviour of the subsidiary absorption signal at fixed pumping frequency, as presented in figure 6. The lower line shows the dependence of the Suhl threshold on H (the so–called *butterfly curve*) [1]. The next line indicates a Hopf bifurcation and corresponds to the onset of auto-oscillations. Further bifurcation lines above separate regimes of different time behaviour, e.g. period doublings, quasiperiodicity, different types of intermittency or chaos. The auto–oscillation frequencies were in the MHz range and changed dramatically on variation of system parameters, thus making the τ adjustment a challenge. For the given setup an intrinsic control loop latency of about 70ns was observed.

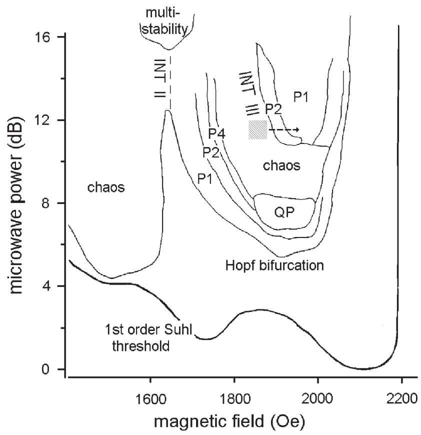

FIG. 6. Experimental bifurcation diagram for high–power ferromagnetic resonance on a YIG sphere ($\nu = 9.39$GHz) with respect to magnetic field H and input microwave power P_{in}. The lowest line indicates the Suhl threshold, the lines above separate regimes of different time behaviour, e.g. period doublings (P2, P4), quasiperiodicity (QP), different types of intermittency (INT II, III) or chaos.

To illustrate the applicability of the delayed feedback control method to complex spin systems, as a first step we considered a *stable* period–2 orbit (figure 7, $K = 0$), which was generated through a period doubling, leaving an unstable period–1 orbit with flipping neighbourhood ($\omega = \pi/T$). This unstable orbit was selected for control. The delay time $\tau = 2.09\mu$s was evaluated from the very sharp and dominating peak in the spectrum. Turning on the feedback and increasing the control amplitude K, we observed a changeover to period–1 (figure 7, $K = 0.2$), while the period–2 component was suppressed by more than 20dB. The vanishing control signal (below a noise level of about 1% of the diode signal) indicated successful control. On further increase of K, the orbit was destabilised again. A widening of the attractor occurred, accompanied by a Hopf bifurcation which resulted in an additional broad peak at about 1.53MHz (figure 7, $K = 0.5$). According to the theoretical expectations, there is a K–window of successful control which is limited at low K–values by a flip bifurcation and at high K–values by a Hopf bifurcation.

In order to extend these control experiments to the chaotic regime we looked for a parameter range where chaos evolves via a period doubling, leading to a flipping neighbourhood ($\omega = \pi/\tau$). However, this period doubling was followed by two Hopf bifurcations making the the situation more complex. A proper starting value for

[1]Here and in the corresponding figures below P_{in} was normalized to the minimum threshold.

the cycle time $\tau = 2.08\mu$s was obtained from the unperturbed spectrum, (figure 8, $K = 0$). The unperturbed spectrum again shows a noisy but pronounced period–2 component. Applying a moderate feedback amplitude ($K = 0.37$), the irregular behaviour was largely suppressed (figure 8). The period–1 peak became rather narrow, the period–2 fluctuations were decreased by about 15dB, while the frequency components which resulted from the Hopf bifurcations were less affected.

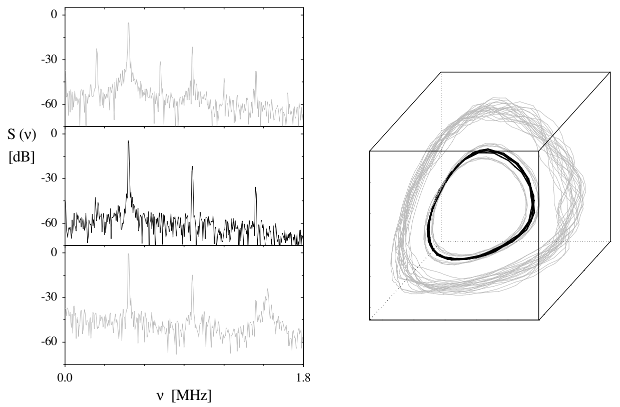

FIG. 7. Suppression of a period–2 orbit (parallel pumping, $\nu = 9.39$GHz, $P_{in} = 13.3$dB, $H = 1613$Oe). L.h.s. top to bottom: stable period–2 orbit ($K = 0$), controlled period–1 orbit ($K = 0.2$), feedback induced torus ($K = 0.5$). R.h.s.: corresponding phase space representations. Note that the stabilised UPO (dark) is located close to the starting period–2 orbit, while for large K an attractor widening occurs.

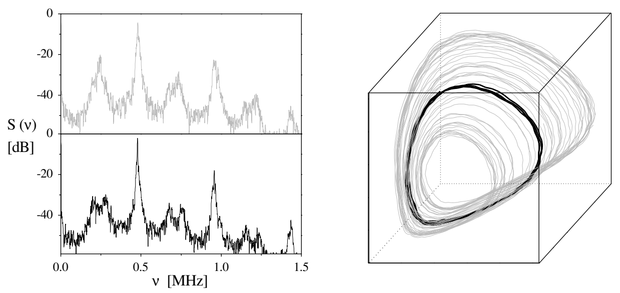

FIG. 8. Suppression of chaos (subsidiary absorption, $\nu = 9.39$GHz, $P_{in} = 8.5$dB, $H = 1865$Oe). L.h.s. top to bottom: chaotic attractor ($K = 0$), stabilised period–1 orbit ($K = 0.37$). R.h.s.: corresponding phase space representations. Note that the stabilised periodic orbit (dark) is embedded in the chaotic attractor.

These experiments show that chaotic spin systems, in spite of their complexity and fast time scale, can be controlled by time–delayed feedback technique. General properties and limitations of this technique, as predicted from a system–independent theory, show up very distinctly in our experimental findings.

ACKNOWLEDGEMENT

The authors are very much indebted to Dr. E. Reibold and D. Reckwerth (TU–Darmstadt) for experimental support and to Prof. E. Schöll (TU–Berlin) and Prof. J. Holyst (TU–Warsaw) for fruitful discussions.

[1] E. Ott, C. Grebogi, and Y. A. Yorke, Phys. Rev. Lett. **64**, 1196 (1990).
[2] *Handbook of Chaos Control*, edited by H. G. Schuster (Wiley–VCH, Berlin, 1999).
[3] R. Bellmann, *Dynamic programming and modern control theory* (Acad. Press, New York, 1965).
[4] K. Ogata, *Modern Control Engineering* (Prentince–Hall, New York, 1997).
[5] K. Pyragas, Phys. Lett. A **170**, 421 (1992).
[6] S. Bielawski, D. Derozier, and P. Glorieux, Phys. Rev. E **49**, R971 (1994).
[7] T. Pierre, G. Bonhomme, and A. Atipo, Phys. Rev. Lett. **76**, 2290 (1996).
[8] J. K. Hale and S. M. V. Lunel, *Introduction to Functional Differential Equations* (Springer, New York, 1993).
[9] M. E. Bleich and J. E. S. Socolar, Phys. Lett. A **210**, 87 (1996).
[10] W. Just, T. Bernard, M. Ostheimer, E. Reibold, and H. Benner, Phys. Rev. Lett. **78**, 203 (1997).
[11] H. Nakajima, Phys. Lett. A **232**, 207 (1997).
[12] W. Just, E. Reibold, K. Kacperski, P. Fronczak, J. Holyst, and H. Benner, Phys. Rev. E **61**, 5045 (2000).
[13] R. Bellmann, *Differential–Difference Equations* (Acad. Press, New York, 1963).
[14] W. Just, E. Reibold, H. Benner, K. Kacperski, F. Fronczak, and J. Holyst, Phys. Lett. A **254**, 158 (1999).
[15] J. E. S. Socolar, D. W. Sukow, and D. J. Gauthier, Phys. Rev. E **50**, 3245 (1994).
[16] S. Bielawski, D. Derozier, and P. Glorieux, Phys. Rev. A **47**, R2492 (1993).
[17] H. G. Schuster and M. B. Stemmler, Phys. Rev. E **56**, 6410 (1997).
[18] W. Just, Physica D **142**, 153 (2000).
[19] K. Pyragas, Phys. Rev. Lett. **86**, 2265 (2001).
[20] A. Kittel, J. Parisi, and K. Pyragas, Phys. Lett. A **198**, 433 (1995).
[21] H. Nakajima, H. Ito, and Y. Ueda, IEICE Trans. Fund. **E80**, 1554 (1997).
[22] W. Just, J. Möckel, D. Reckwerth, E. Reibold, and H. Benner, Phys. Rev. Lett. **81**, 562 (1998).
[23] L. Collatz, ZAMM **25/27**, 60 (1947).
[24] W. Just, D. Reckwerth, E. Reibold, and H. Benner, Phys. Rev. E **59**, 2826 (1999).
[25] M. C. Cross and P. C. Hohenberg, Rev. Mod. Phys. **65**, 851 (1993).
[26] F. Rödelsperger, *Chaos und Spinwelleninstabilitäten* (Harri Deutsch, Frankfurt, 1994).